Table 5. Relationship between first (GVHD-induced) and second (rescue) donors in graft-versus-GVHD treatment

No.	First donor	Second donor	Relationship of 2 donors (second to first donors)	HLA disparity in the direction of 1st to 2nd donors	GVH-target HLA antigens in 2nd donor*	Engraftment of rescue grafts
14	first son	second son	HLA-matched sibling	0	–	+
15	younger sister	youngest sister	HLA-matched sibling	0	–	+
17	brother	sister	HLA-matched sibling	0	–	+
1	mother	sister	Daughter and mother	2	–	+
9	sister	mother	Mother and daughter	3	–	+
10	brother	mother	Mother and son	3	–	+
16	UCB	son	Unrelated	2	–	+
5	first son	second son	HLA-haploidentical sibling	3	A24B48DR14	+
6	mother	brother	Son and mother	2	A26B59	+
7	mother	sister	Daughter and mother	2	B7DR1	+
11	brother	mother	Mother and son	2	B52DR15	+/–†
12	son	brother	Uncle and nephew	2	B54DR4	–
8	father	mother	Spouse	5	A11B35DR4	–
13	father	mother	Spouse	6	A33B44DR13	–

*HLA determinants of 2nd donors that could be major targets for GVH reaction in first (GVHD-induced) transplantation.
†The patient rejected the first rescue transplantation, but achieved engraftment of the second rescue transplantation.

usually tolerate an intensified conditioning treatment. However, as shown in our murine BMT model, recipients with severe GVHD were in a profoundly immunosuppressive state as a result of GVHD-related activation-induced cell death [27,28] and, therefore, with the help of unmanipulated (T-cell replete) grafts, could easily accept second allografts, even under minimal conditioning treatment, which was advantageous for recipients with serious organ damage.

Regarding GVHD induced by second allogeneic grafts, we demonstrated that second GVHD could be suppressed by conventional GVHD prophylaxis consisting of FK506 and a small dose of mPSL. This was fully expected because, in the unmanipulated HLA-haploidentical reduced-intensity SCT that we recently developed, using a conditioning treatment consisting of fludarabine + busulfan + ATG, and GVHD prophylaxis consisting of FK506 + mPSL 1 mg/kg, the actual incidence of GVHD was only 10% [13]. We consider that, in addition to in vivo T-cell purging by ATG, reduced-intensity conditioning, and a small dose of mPSL effectively suppressed inflammatory cytokine production in the transplantation period, which was shown to be closely involved in the pathophysiology of GVHD [29]. The molecular and cellular mechanisms of the high resistance to GVHD development have not been fully determined: however, in our murine studies, significantly reduced interferon-γ levels and a significantly increased percentage of $CD3^+CD4^+foxp3^+$ cells [30,31] were observed in day 7 spleens of second rescue BMT recipients compared with recipients of first BMT with severe GVHD. In addition, antigen-presenting cells (APCs) in the recipient spleen were found to have already been replaced by those of first-donor origin at the time of the second BMT. When APCs are replaced with first donor-derived cells from host cells, the first donor APCs need to cross-present host antigens to second donor T cells to induce GVHD; however, it was reported using major histocompatibility complex–matched, minor antigen-mismatched, murine BMT systems that this cross-presentation was insufficient to induce GVHD [32]. Although the present study includes mostly HLA-mismatched donor/recipient combinations, the limited ability of first donor-derived APCs to cross-present host antigens is considered to reduce the magnitude of the GVH reaction, at least compared with the first transplantation, in which host-type APCs directly present host antigens.

For successful graft-versus-GVHD treatment, engraftment of the rescue donor graft was mandatory in our murine model in which immunosuppressive agents were not used. In the present clinical study, even in patients who rejected the rescue graft, some GVHD symptoms improved within a week after the second transplantation because of conditioning treatment, including immunosuppressive agents and possibly because of the alloreactive response of second donor grafts to dampen first donor lymphocytes. Although these effects may have potential to completely control GVHD coupled with GVHD prophylaxis after second transplantation, as observed in patient no. 11, basically as long as the alloresponse from first donor-derived lymphocytes is maintained, GVHD symptoms continue or are aggravated, as shown in most patients who rejected second grafts. In fact, 8 of the 11 patients achieving rescue donor engraftment had a complete response, and 6 of the 8 patients survived without GVHD symptoms, with a median follow-up of 2128 days. These results strongly suggest, also in humans, that the engraftment of second donor grafts contributes to enduring control of GVHD and longer survival of patients with severe, refractory GVHD. Regarding HLA disparity between the first and second (rescue) donors, when rescue donors did not have HLA determinants that could be major targets for the GVH reaction in transplantation inducing GVHD, no rejection occurred (Table 5). As the extent

of HLA disparity in the direction of the first to second donor became greater, rejection tended to occur more frequently. When the 2 donors were HLA-matched siblings, 100% rescue donor chimerism was gradually achieved over 2 to 3 months.

Furthermore, as suggested in our murine model, the timing of rescue transplantation was another key factor for obtaining a positive graft-versus-GVHD effect. In particular, graft-versus-GVHD treatment in the late stage of GVHD is not effective. When organ damage due to GVHD proceeds fully, although the cell components involved in GVHD are all eliminated, recovery from severe organ damage is difficult, as shown by the lack of long-term survivors among recipients with a low PS score ≤20%. Thus, graft-versus-GVHD treatment may be started as one of the treatments for steroid-refractory GVHD before patients are heavily treated.

As patients did not show relapse of the original disease after successful graft-versus-GVHD treatment, and the majority of GVHD patients treated by autologous SCT had a relapse of the original disease [8–10], this strongly suggests GVL effects of second rescue allografts. In autologous transplant settings for GVHD, autografts can reintroduce malignant cells into the recipients in addition to the absence of GVL effects. Furthermore, in rescue transplantation of GVHD by allogeneic grafts, there is a possibility that malignant cells may have been eliminated by allogeneic NK cells as ATG was integrated into the conditioning treatment [33]. Thus, graft-versus-GVHD treatment has a unique feature in that it exerts GVL effects together with treating GVHD, which indicates the achievement of separating GVL from GVHD, a goal in allogeneic SCT.

We have proposed here the novel concept of graft-versus-GVHD and clinically showed that, using reduced-intensity conditioning and T-cell–replete grafts mostly from an HLA-mismatched donor, the second allogeneic SCT succeeded in eliminating harmful lymphocytes responsible for GVHD without the new development of GVHD. Thus, this graft-versus-GVHD strategy may be a promising treatment for refractory GVHD, although our results will have to be confirmed in a large-scale study.

Acknowledgments

We thank Aya Yano and Kimiko Yamamoto for their excellent technical assistance in donor/recipient chimerism analysis.

Conflict of interest disclosure

No financial interest/relationships with financial interest relating to the topic of this article have been declared.

References

1. Gratwohl A, Brand R, Apperley J, et al. Graft-versus-host disease and outcome in HLA-identical sibling transplantations for chronic myeloid leukemia. Blood. 2002;100:3877–3886.
2. Teshima T, Ferrara JL. Understanding the alloresponse: new approaches to graft-versus-host disease prevention. Semin Hematol. 2002;39:15–22.
3. Le Blanc K, Frassoni F, Ball L, et al. Mesenchymal stem cells for treatment of steroid-resistant, severe, acute graft-versus-host disease: a phase II study. Lancet. 2008;371:1579–1586.
4. Bolanos-Meade J, Jacobsohn DA, Margolis J, et al. Pentostatin in steroid-refractory acute graft-versus-host disease. J Clin Oncol. 2005;23:2661–2668.
5. Patriarca F, Sperotto A, Damiani D, et al. Infliximab treatment for steroid-refractory acute graft-versus-host disease. Haematologica. 2004;89:1352–1359.
6. Przepiorka D, Kernan NA, Ippoliti C, et al. Daclizumab, a humanized anti-interleukin-2 receptor alpha chain antibody, for treatment of acute graft-versus-host disease. Blood. 2000;95:83–89.
7. Antin JH, Chen AR, Couriel DR, Ho VT, Nash RA, Weisdorf D. Novel approaches to the therapy of steroid resistant acute graft-versus-host disease. Biol Blood Marrow Transplant. 2004;10:655–668.
8. Taniguchi Y, Ikegame K, Yoshihara S, Sugiyama H, Kawase I, Ogawa H. Treatment of severe life-threatening graft-versus-host disease by autologous peripheral blood stem cell transplantation using a non-myeloablative preconditioning regimen. Haematologica. 2003;88:ELT06.
9. Orchard K, Blackwell J, Chase A, et al. Autologous peripheral blood cell transplantation as treatment of life-threatening GVHD. Blood. 1996;88:421a [abstract].
10. Passweg JR, Orchard K, Buergi A, et al. Autologous/syngeneic stem cell transplantation to treat refractory GvHD. Bone Marrow Transplant. 2004;34:995–998.
11. Taniguchi Y, Yoshihara S, Hoshida Y, et al. Recovery from established graft-vs-host disease achieved by bone marrow transplantation from a third-party allogeneic donor. Exp Hematol. 2008;36:1216–1225.
12. Burt RK, Verda L, Oyama Y, Statkute L, Slavin S. Non-myeloablative stem cell transplantation for autoimmune diseases. Springer Semin Immunopathol. 2004;26:57–69.
13. Ogawa H, Ikegame K, Yoshihara S, et al. Unmanipulated HLA 2-3 antigen-mismatched (haploidentical) stem cell transplantation using nonmyeloablative conditioning. Biol Blood Marrow Transplant. 2006;12:1073–1084.
14. Deeg HJ. How I treat refractory acute GVHD. Blood. 2007;109:4119–4126.
15. Ogawa H, Ikegame K, Kaida K, et al. Unmanipulated HLA 2-3 antigen-mismatched (haploidentical) bone marrow transplantation using only pharmacological GVHD prophylaxis. Exp Hematol. 2008;36:1–8.
16. Ogawa H, Ikegame K, Kawakami M, et al. Powerful graft-versus-leukemia effects exerted by HLA-haploidentical grafts engrafted with a reduced-intensity regimen for relapse following myeloablative HLA-matched transplantation. Transplantation. 2004;78:488–489.
17. Ogawa H, Soma T, Hosen N, et al. The combination of tacrolimus, methotrexate, and methylprednisolone completely prevents acute graft-versus-host disease (GVHD) but not chronic GVHD in unrelated bone marrow transplantation. Transplantation. 2002;74:236–243.
18. Siegert W, Josimovic-Alasevic O, Schwerdtfeger R, et al. Soluble interleukin 2 receptors after bone marrow transplantation. Bone Marrow Transplant. 1990;6:97–101.
19. Glucksberg H, Storb R, Fefer A, et al. Clinical manifestations of graft-versus-host diseases in human recipients of marrow from HLA matched sibling donors. Transplantation. 1974;18:295–304.
20. Filipovich AH, Weisdorf D, Pavletic S, et al. National Institutes of Health consensus development project on criteria for clinical trials in chronic graft-versus-host disease: I. Diagnosis and staging working group report. Biol Blood Marrow Transplant. 2005;11:945–956.
21. Przepiorka D, Weisdorf D, Martin P, et al. 1994 Consensus Conference on Acute GVHD Grading. Bone Marrow Transplant. 1995;15:825–828.

22. Zeigler ZR, Shadduck RK, Nemunaitis J, Andrews DF, Rosenfeld CS. Bone marrow transplant-associated thrombotic microangiopathy: a case series. Bone Marrow Transplant. 1995;15:247–253.
23. Nishida T, Hamaguchi M, Hirabayashi N, et al. Intestinal thrombotic microangiopathy after allogeneic bone marrow transplantation: a clinical imitator of acute enteric graft-versus-host disease. Bone Marrow Transplant. 2004;33:1143–1150.
24. Tamaki H, Ikegame K, Kawakami M, et al. Successful engraftment of HLA-haploidentical related transplants using nonmyeloablative conditioning with fludarabine, busulfan and anti-T-lymphocyte globulin. Leukemia. 2003;17:2052–2054.
25. Peters CE, Clarke E, Lansdorp PM, Eaves AC, Thomas TE. Non-magnetic extensive enrichment of progenitors directly from whole cord blood. Blood. 1999;94:570a.
26. MacMillan ML, Weisdorf DJ, Wagner JE, et al. Response of 443 patients to steroids as primary therapy for acute graft-versus-host disease: comparison of grading systems. Biol Blood Marrow Transplant. 2002;8:387–394.
27. Brochu S, Rioux-Masse B, Roy J, Roy DC, Perreault C. Massive activation-induced cell death of alloreactive T cells with apoptosis of bystander postthymic T cells prevents immune reconstitution in mice with graft-versus-host disease. Blood. 1999;94:390–400.
28. Lin MT, Tseng LH, Frangoul H, et al. Increased apoptosis of peripheral blood T cells following allogeneic hematopoitic cell transplantation. Blood. 2000;95:3832–3839.
29. Ferrara JL, Levy R, Chao NJ. Pathophysiology mechanism of acute graft-vs.-host disease [review]. Biol Blood Marrow Transplant. 1999;5:347–356.
30. Miura Y, Thoburn CJ, Bright EC, et al. Association of Foxp3 regulatory gene expression with graft-versus-host disease. Blood. 2004;104: 2187–2193.
31. Sakaguchi S. Naturally arising Foxp3-expressing CD25+CD4+ regulatory T cells in immunological tolerance to self and non-self. Nat Immunol. 2005;6:345–352.
32. Shlomchik WD, Couzens MS, Tang CB, et al. Prevention of graft versus host disease by inactivation of host antigen-presenting cells. Science. 1999;285:412–415.
33. Giebel S, Locatelli F, Lamparelli T, et al. Survival advantage with KIR ligand incompatibility in hematopoietic stem cell transplantation from unrelated donors. Blood. 2003;102:814–819.

Notch2 and Immune Function

Mamiko Sakata-Yanagimoto and Shigeru Chiba

Abstract Notch2 is expressed in many cell types of most lineages in the hematolymphoid compartment and has specific roles in differentiation and function of various immune cells. Notch2 is required for development of splenic marginal zone B cells and regulates differentiation of dendritic cells (DCs) in the spleen. Notch2 appears to play some specific roles in the intestinal immunity, given that the fate of mast cells and a subset of DCs is regulated by Notch2 in the intestine. Notch2 also has important roles in helper T cell divergence from na CD4 T cells and activation of cytotoxic T cells. Moreover, recent genetic evidence suggests that both gain-and loss-of-function abnormalities of Notch2 cause transformation of immune cells. Inactivating mutations are found in Notch2 signaling pathways in chronic myelomonocytic leukemia, while activating mutations are found in mature B cell lymphomas, which reflects the role of Notch2 in the developmental process of these cells.

Contents

M. Sakata-Yanagimoto · S. Chiba (✉)
Department of Hematology, Faculty of Medicine, University of Tsukuba,
1-1-1 Tennodai, Tsukuba, Ibaraki 305-8575, Japan
e-mail: schiba-tky@umin.net

Current Topics in Microbiology and Immunology (2012) 360: 151–161
DOI: 10.1007/82_2012_235

Published Online: 14 June 2012

1 Introduction

The expression pattern of Notch1, Notch2, Notch3, and Notch4 varies from one cell type to another. Notch2 plays specific roles in the immune compartment independently of and cooperatively with Notch1 and Notch3. In this chapter, we mostly focus on evidence based on mouse genetic studies regarding Notch2 functions in immune cells. In the last part, we discuss the involvement of Notch2 in neoplastic transformation in conjunction with human hematologicmalignancies.

2 Notch2 Signaling in Marginal Zone B Cell Development

Mature splenic B cells are mainly divided into 2 types of B cells, follicular B (FOB) cells and marginal zone B (MZBs) cells (Martin and Kearney 2002). FOB cells are one of the main effectors of acquired immunity, able to respond to a large variety of antigens, while MZB cells can only elicit an immune response to a limited number of antigens. Immature B cells, developing from hematopoietic stem cells (HSCs) in the bone marrow, migrate to the spleen, and differentiate first into T1 (type1) transitional B cells (characterized by: IgM^{hi} IgD^{lo} $CD21^{lo}$), before differentiating into T2 (type2) transitional B cells (IgM^{hi} IgD^{hi} $CD21^{int}$ $CD23^{hi}$) (Loder et al. 1999). These progenitors further differentiate into the two types of B cells, MZB cells (IgM^{hi} IgD^{lo} $CD21^{hi}$ $CD23^{lo}$) and FOB cells (IgM^{lo} IgD^{hi} $CD21^{int}$ $CD23^{hi}$) (Martin and Kearney 2002). Conditional inactivation of *Notch2* in the B cell lineage results in defective MZB cell development, while FOB cell development is unaffected (Saito et al. 2003), which is basically consistent with the phenotype of *RBP-J* conditional knockout mice (Tanigaki et al. 2002). The cleaved Notch-RBP-J activator complex contains at least one out of three family members of the mastermind-like proteins (MAML1-3). Mastermind-like1 (MAML1) plays an essential role in MZB cell development, which is why MZB cells are lacking in *MAML1*-null mice (Wu et al. 2007; Oyama et al. 2007). Among Notch ligands, Delta-like 1 (Dll1) is responsible for MZB cell development, based on the fact that *Dll1* deletion using the Mx-Cre *loxP* system leads to loss of MZB cells (Hozumi et al. 2004; Sheng et al. 2008). Several lines of evidence indicate that loss of *Dll1* expression on nonhematopoietic cells causes MZB cell defects (Hozumi et al. 2004; Sheng et al. 2008; Tan et al. 2009). However, the exact cell types through which Dll1-induced Notch2 signaling triggers MZB development remains to be elucidated. The essential role of Notch signaling in MZB cell development is further proven by a number of other gene-targeted mice in which

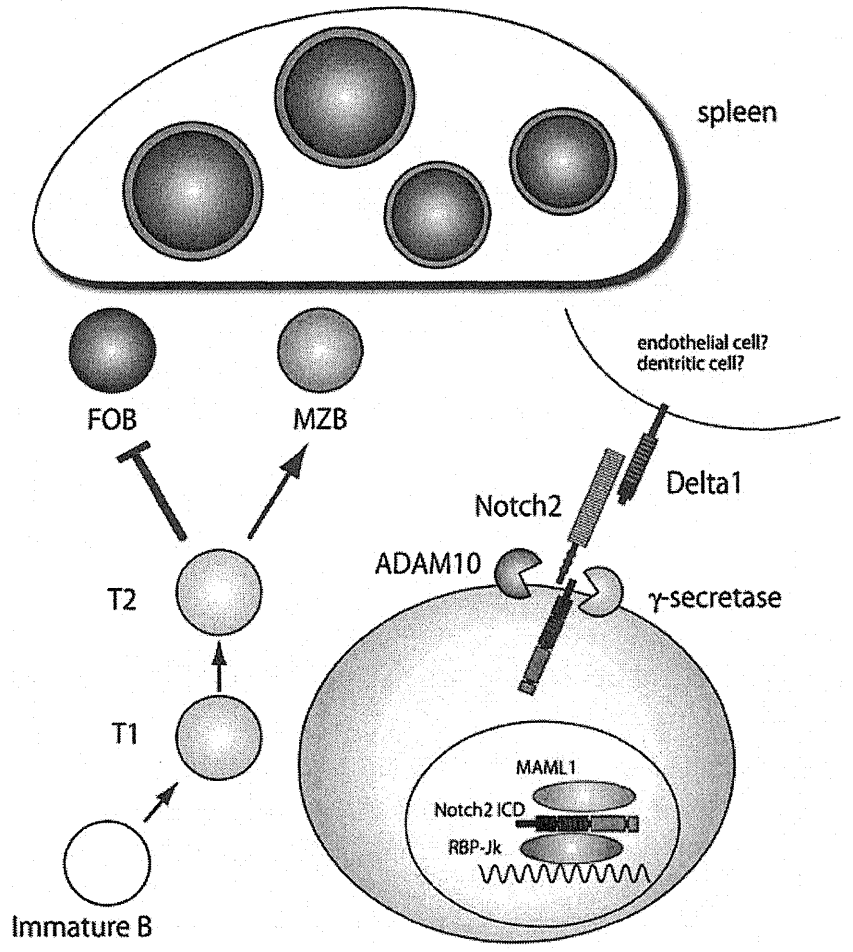

Fig. 1 Notch2 regulates marginal zone B cell development. Dll1 engagement of the Notch2 receptor expressed on splenic immature B cells initiates the Notch2 signaling cascade through ADAM10-mediated cleavage. This results in the formation of Notch-RBP-J-MAML1 proteins, which regulates gene expression and skews the differentiation program toward MZB cells rather than FOB cells

genes of the Notch signaling cascade were inactivated. Mind bomb (Mib), an E3 ubiquitin ligase, activates Notch signaling through endocytosis of Notch ligands. Deletion of *Mib1* in nonhematopoietic cells recapitulates defects in MZBs, whereas deletion in hematopoietic cells resulted in MZB levels that were comparable to control mice (Song et al. 2008).

Deletion of *ADAM10*, which encodes a matrix metalloprotease that processes the extracellular domain of the Notch receptor after ligand binding, also results in defects in MZB cells (Gibb et al. 2010). In contrast, deletion of *Msx2-interacting nuclear target protein* (*MINT*), which is a repressor of RBP-J mediated transcriptional activity and thus considered to be a negative regulator for Notch signaling, showed decreased numbers of FOB cells and increased numbers of MZB cells (Kuroda et al. 2003). Notch receptors can be modified by fringe glycosyl transferases. Lunatic and manic fringe were shown to cooperatively enhance Dll1-Notch2 interaction, and thereby induce MZB development (Tan et al. 2009).

Taken together, these data suggest that Dll1 engagement of the Notch2 receptor expressed on splenic immature B cells initiates the Notch2 signaling cascade through ADAM10-mediated cleavage. This results in the formation of a multi-protein complex including Notch-RBP-J-MAML1 proteins, which regulates gene expression and thereby skews the differentiation program toward MZB cells rather than FOB cells (Fig. 1).

3 Notch2 Signaling in Peripheral T Cell Differentiation and Activation

Signaling through Notch1 has been proven to be among the most important systems for immature T cell differentiation in the thymus (Radtke et al. 1999). During T cell differentiation, Notch signaling is also an essential component for functional maturation and activation of peripheral T cells, in which Notch2 appears to be among the main players (Maekawa et al. 2008). Notch2 expression is increased along with activation of CD8+ cytotoxic T lymphocytes (CTL) (Maekawa et al. 2008). CTLs of both *Notch2* and *RBP-J* conditional knockout mice show an impaired activation potential in vitro as well as in vivo (Maekawa et al. 2008). Cleaved Notch2 (N2IC) directly interacts with CREB and p300 and binds to the promoter of the granzyme B gene, an effector molecule of CTL (Maekawa et al. 2008). Conditional inactivation of *Notch2* in CD8+ T cells results in a decreased antitumor response (Sugimoto et al. 2010). Notch1 appears to be dispensable for an efficient CTL response given the fact that deletion of *Notch1* in CD8+ T cells shows an antitumor response comparable to control mice (Sugimoto et al. 2010). However, this view was recently challenged by a report showing that Notch1 also directly controls main players of CTL, including Eomes, perforin, and granzyme B (Cho et al. 2009).

Notch2/Notch1 double deficient animals reveal impaired differentiation of na CD4+ T cells toward helper T2 (Th2) cells. Notch was shown to directly regulate the transcription of the transcription factor GATA3, and the cytokine interleukin-4 (IL-4) (Amsen et al. 2004, 2007; Fang et al. 2007), both of which are important mediators of Th2 differentiation. *RBP-J* deficient animals recapitulate the phenotype observed in *Notch2/Notch1* deficient animals indicating that this process is mediated through canonical Notch signaling (Amsen et al. 2004). The role of Notch signaling in Th1 differentiation is less clear. Several reports demonstrated that Th1 differentiation is augmented by Notch signaling (Maekawa et al. 2003; Sun et al. 2008); however, a Th1 response is maintained in *Notch2/Notch1* double deficient, and *RBP-J* deficient animals (Amsen et al. 2004), as well as in mice expressing a dominant negative *MAML1* (Tu et al. 2005), questioning the importance of Notch signaling in Th1 differentiation.

With certainty, it can thus be summarized that Notch2 signaling induces cytotoxic T cell differentiation and activation, and that Notch1 and Notch2 concordantly induce Th2 cell differentiation.

4 Notch2 Signaling in Mast Cells

Mast cells arise from HSCs in the bone marrow, migrate to peripheral tissues as immature progenitors, where they subsequently differentiate into mature mast cells (Galli et al. 2005). However, the detailed process of their development is still disputed. Mast cells can be generated in vitro by culturing mouse bone marrow cells with a defined cocktail of cytokines. This in vitro system allows to partially mimic the physiologic development of mast cells. Notch2 signaling instructs myeloid progenitors to adopt a mast cell fate as opposed to differentiate into neutrophils or macrophages, through the coordinated regulation of *Hes1* and *GATA3* (Sakata-Yanagimoto et al. 2008). Mast cells are divided into two subtypes; mucosal and connective tissue type mast cells (Gurish and Boyce 2006; Miller and Pemberton 2002). Each subtype features specific mast-cell proteases (mMCP) (Miller and Pemberton 2002). Notch2 signaling skews cultured mast cells toward the mucosal type rather than connective tissue type (M.S.-Y. and S.C., unpublished data). The *Strongyloides venezuelensis* (*SV*) infection model is useful for analyzing mast cell-mediated mucosal immunity (Maruyama et al. 2000). This nematode evokes intraepithelial mast cell hyperplasia in the small intestine (Maruyama et al. 2000). *Notch2*-null mice show impaired expulsion of *SV*, possibly because of a delayed mast cell progenitor production in the bone marrow, impaired migration of mast cells from the lamina propria to the intraepithelium of the intestine, and impaired activation of intestinal mast cells (Sakata-Yanagimoto et al. 2011). The number and distribution of connective tissue-type mast cells are normal in *Notch2*-null mice (Sakata-Yanagimoto et al. 2011), suggesting that Notch2 signaling is specifically required for proper migration and activation of intestinal mast cells.

5 Notch2 Signaling in Dendritic Cells

Dentritic cells (DCs) initiate immune responses by presenting antigen to na T cells (Steinman and Idoyaga 2010). DCs arise from common bone marrow progenitors that can give rise to both DCs and macrophages (Steinman and Idoyaga 2010). DCs comprise two subclasses, i.e., the so-called plasmacytoid DCs and classical DCs. Classical DCs residing in the spleen are further classified into two main subsets; CD8+CD11b− DCs which mediate cross-presentation to cytotoxic T cells via MHC class I pathway (Dudziak et al. 2007; den Haan et al. 2000) and CD8−CD11b+ DCs which preferentially present MHC class II restricted antigens to CD4+ helper T cells (Dudziak et al. 2007). CD8−CD11b+ DCs are mainly localized in the marginal zone, adjacent to the Dll1-expressing cells (Caton et al. 2007). CD11b+ DCs in the lamina propria of the intestine contain two distinct subsets; CD11b+CD103+ DCs and CD11b+CD103− DCs. CD11b+CD103+ DCs migrate to mesenteric lymph nodes and are presumed to have antigen presenting potential to helper T cells (Denning et al. 2011; Bogunovic et al. 2009).

DC-specific deletion of either *Notch2* or *RBP-J* impairs the development of CD8−CD11b+ DCs in the spleen (Caton et al. 2007; Lewis et al. 2011). CD8+ DCs are also decreased by deletion of *Notch2* but are not affected by the deletion of *RBP-J* (Caton et al. 2007; Lewis et al. 2011). Splenic CD11b+ DCs are divided into two subsets according to the expression levels of Esam and Cx3cr1 (Lewis et al. 2011). CD11b+Esam^{high}Cx3cr1^{low} but not CD11b+Esam^{low}Cx3cr1^{high} DCs are almost abrogated by deletion of either *Notch2* or *RBP-J* (Lewis et al. 2011). CD11b+Esam^{high}Cx3cr1^{low} cells are required for proper priming of T cells in the spleen, which are reduced in *RBP-J*-null mice (Lewis et al. 2011).

Notch2 selectively controls CD11b+CD103+ DCs in the lamina propria of the intestine as well as those that migrate toward mesenteric lymph nodes, which in turn are important for supporting IL-17 producing CD4+ T cells. CD11b+CD103+ DCs are not affected by the inactivation of *RBP-J* (Lewis et al. 2011).

Taken together, Notch2 regulates tissue-specific subsets of DCs in the spleen and in the intestine. Notch2 function might be partly mediated by a RBP-J independent/noncannonical pathway.

6 Notch2 Signaling in Hematopoietic Stem Cells

Notch signaling plays an essential role in self-renewal of stem cells as well as in the growth and differentiation of diverse progenitors within various organs. In contrast, the role of Notch signaling in self-renewal of HSC has been disputed over the years. Early in vitro gain-of-function experiments, such as introduction of a constitutive active form of Notch (Varnum-Finney et al. 2000; Stier et al. 2002) or the transcription factor Hes1 (Kunisato et al. 2003), and stimulation of HSCs with cell-surface expressed ligands or ligand-immunoglobulin chimeric proteins (Karanu et al. JEM 2000; Ohisi et al. JCI 2002; Suluki et al. Stem cells 2006), indicated that Notch signaling supports self-renewal of HSCs and has a role in HSC expansion. On the contrary, several loss-of-function experiments suggest that Notch signaling is dispensable for maintenance of HSCs. HSCs lacking *RBP-J* and those expressing dominant negative *MAML1*, a potent inhibitor of the Notch transcriptional complex, achieve long-term reconstitution comparable to wild-type HSCs, when transplanted into irradiated mice (Maillard et al. 2008). The reconstitution potential of HSCs null for both *Notch1* and *Jagged1* was shown to be comparable to that of wild-type HSCs (Mancini et al. 2005).

However, recently, such negative findings were partially challenged. At a very early time point after treatment with 5-fluorouracil, the number of multipotent progenitors (MPPs) was decreased in *Notch2*-null mice, compared to that in control mice (Varnum-Finney et al. 2011). Similarly, shortly after transplantation, both MPPs and long-term HSCs were decreased in *Notch2*-null BM transplanted mice (Varnum-Finney et al. 2011).

In summary, these data suggest that although Notch signaling is dispensable for homeostasis of HSCs, in challenge and stress situations signaling through Notch2 seems to play a role in the process of HSCs expansion.

7 Notch2 Signaling in Transformation of Blood Cells

7.1 Notch2 Mutations in B Cell Lymphomas

Notch1 is among the most important molecules for physiologic development of T cells (Radtke et al. 1999), and Notch2 is indispensable for MZB cell development (Saito et al. 2003) as described above. Discovery of hyperactivation of Notch1 and Notch2 through gain-of-function mutations in immature T cell neoplasms (Weng et al. 2004) (T cell acute lymphoblastic leukemia or T-ALL in humans) and in subtypes of mature B cell neoplasms (Lee et al. 2009; Troen et al. 2008), respectively, appears to echo the physiologic roles of these molecules in specific lineages and differentiation stages. Those mutations are concentrated in the extracellular heterodimerization (HD) domain and the intracellular proline-, glutamic acid-, serine-, and threonine-rich (PEST) domain of *Notch1* in T-ALL (Weng et al. 2004), and only in the PEST domain of *Notch2* in mature B cell lymphomas (Lee et al. 2009; Troen et al. 2008). The distribution of mutations suggests that hyperactivation of Notch2 signaling in B cell lymphomas still requires binding of the ligand, whereas mutations within the HD domain of *Notch1* in T-ALL results in ligand independent activation of Notch1 signaling. In contrast to the fact that *Notch1* mutations are found in approximately 50 % of T-ALL cases (Weng et al. 2004), *Notch2* mutations were identified in only five out of 63 cases (8 %) of diffuse B-cell lymphoma (Lee et al. 2009) and in two out of 41 cases (5 %) of MZB cell lymphoma (Troen et al. 2008).

The relationship between B cell development and gain-of-function mutations in Notch2 is not as clear as in the context of T cell development and Notch1 mutations. Genetic evidence described above strongly suggests an oncogenic role of deregulated Notch2 in B lineage transformations. On the contrary, there has been a series of reports describing the tumor suppressive function of Notch signaling in B lineage cells, particularly in B-cell lymphoblastic leukemia (B-ALL) (Zweidler-McKay et al. 2005; Kannan et al. 2011), although loss-of-function mutations have not been found in the Notch2 signaling pathway. Integrating these pieces of information, it seems likely that Notch2 signaling can context dependently promote or suppress growth of B lineage cells. Another complexity was recently added by the identification of Notch1 mutations through the genome-wide screening of patient samples suffering from chronic lymphocytic leukemia (Puente et al. 2011), a type of intermediately mature B cell neoplasm and mantle cell lymphoma (Kridel et al. 2012), another type of mature B neoplasms.

7.2 Notch2 Signaling in Myeloid Neoplasms

Recently, Notch signaling was proven to function as a tumor-suppressor in chronic myelomonocytic leukemia (CMML) (Klinakis et al. 2011); several components of the Notch pathway, including *Nicastrin* (*NCSTN*), *APH1A*, *MAML1*, and *Notch2*

Table 1 Role of Notch signaling as tumor activator or tumor suppressor in hematopoietic leukemia/lymphoma

	Gain-of-function			Loss-of-function	
	T	B	M	B	M
Notch1	T-ALL	CLL	AML	(B-ALL)[a]	
	ATL	MCL			
		DLBCL			
Notch2		MZB lymphoma			CMML
		DLBCL			

T-ALL, T-cell acute lymphocytic leukemia; ATL, adult T-cell leukemia/lymphoma; CLL, chronic lymphocytic leukemia; MCL, mantle cell lymphoma; DLBCL, diffuse large B-cell lymphoma; MZB lymphoma, marginal zone B-cell lymphoma; AML, acute myeloid leukemia; B-ALL, B-cell acute lymphocytic leukemia; CMML, chronic myelomonocytic leukemia

[a] Loss-of-function mutations in Notch signal components have not been found in B-ALL

itself were found to be mutated and defective in CMML patients. This conclusion is also supported by the phenotype of mice lacking *NCSTN*, a component of γ-secretase, as well as that of *Notch1*-, *Notch2*-, and *Notch3*- triple null mice (Klinakis et al. 2011). These animals show enhanced granulocyte-monocyte progenitor potential and develop a fatal CMML-like disease (Klinakis et al. 2011). On the contrary, activating mutations of Notch1 were found in acute myeloid leukemia, a precursor myeloid neoplasms, though the frequency is less than 1 % (Wouters et al. 2007; Fu et al. 2006). Thus, as is the case of B cell malignancies, Notch signaling can function as either tumor promoter or suppressor within myeloid neoplasms.

These oncogenic and tumor suppressive functions of Notch1 and Notch2 signaling in T cell, B cell, and myeloid lineages have been summarized in Table 1. Knowledge about this area will expand rapidly in the very near future using current sequencing technology.

8 Conclusion

Signaling through Notch2 has an essential role in two major cell types present in the marginal zone of the spleen, splenic MZB cells, and splenic DCs. Notch2 signaling also mediates intestinal immunity by regulating development and localization of intestinal DCs and mast cells, and development of helper T cells and CTLs. Genetic and biologic evidence indicates that abnormal Notch2 signaling is involved in transformation of immune cells, although its functions appear to be bivalent; oncogenic signaling for mature B neoplasms and tumor suppressive signaling for mature myeloid neoplasms. The reason of specificity and non-redundant functions of Notch2 in the immune system may be partly attributed to the differences in expression patterns among Notch family genes, although this issue needs to be elucidated in more detail in future studies.

References

Amsen D, Blander JM, Lee GR, Tanigaki K, Honjo T, Flavell RA (2004) Instruction of distinct CD4 T helper cell fates by different notch ligands on antigen-presenting cells. Cell 117(4):515–526

Amsen D, Antov A, Jankovic D et al (2007) Direct regulation of Gata3 expression determines the T helper differentiation potential of Notch. Immunity 27(1):89–99

Bogunovic M, Ginhoux F, Helft J et al (2009) Origin of the lamina propria dendritic cell network. Immunity 31(3):513–525

Caton ML, Smith-Raska MR, Reizis B (2007) Notch-RBP-J signaling controls the homeostasis of CD8− dendritic cells in the spleen. J Exp Med 204(7):1653–1664

Cho OH, Shin HM, Miele L et al (2009) Notch regulates cytolytic effector function in CD8+ T cells. J Immunol 182(6):3380–3389

den Haan JM, Lehar SM, Bevan MJ (2000) CD8(+) but not CD8(−) dendritic cells cross-prime cytotoxic T cells in vivo. J Exp Med 192(12):1685–1696

Denning TL, Norris BA, Medina-Contreras O et al (2011) Functional specializations of intestinal dendritic cell and macrophage subsets that control Th17 and regulatory T cell responses are dependent on the T cell/APC ratio, source of mouse strain, and regional localization. J Immunol 187(2):733–747

Dudziak D, Kamphorst AO, Heidkamp GF et al (2007) Differential antigen processing by dendritic cell subsets in vivo. Science 315(5808):107–111

Fang TC, Yashiro-Ohtani Y, Del Bianco C, Knoblock DM, Blacklow SC, Pear WS (2007) Notch directly regulates Gata3 expression during T helper 2 cell differentiation. Immunity 27(1):100–110

Fu L, Kogoshi H, Nara N, Tohda S (2006) NOTCH1 mutations are rare in acute myeloid leukemia. Leuk Lymphoma 47(11):2400–2403

Galli SJ, Nakae S, Tsai M (2005) Mast cells in the development of adaptive immune responses. Nat Immunol 6(2):135–142

Gibb DR, El Shikh M, Kang DJ et al (2010) ADAM10 is essential for Notch2-dependent marginal zone B cell development and CD23 cleavage in vivo. J Exp Med 207(3):623–635

Gurish MF, Boyce JA (2006) Mast cells: ontogeny, homing, and recruitment of a unique innate effector cell. J Allergy Clin Immunol 117(6):1285–1291

Hozumi K, Negishi N, Suzuki D et al (2004) Delta-like 1 is necessary for the generation of marginal zone B cells but not T cells in vivo. Nat Immunol 5(6):638–644

Karanu FN et al. (2000) The notch ligand Jagged-1 represents a novel growth factor of human hematopoietic stem cells. JEM 192 (9) 1365–1372

Kannan S, Fang W, Song G et al (2011) Notch/HES1-mediated PARP1 activation: a cell type-specific mechanism for tumor suppression. Blood 117(10):2891–2900

Klinakis A, Lobry C, Abdel-Wahab O et al (2011) A novel tumour-suppressor function for the Notch pathway in myeloid leukaemia. Nature 473(7346):230–233

Kridel R, Meissner B, Rogic S et al (2012) Whole transcriptome sequencing reveals recurrent NOTCH1 mutations in mantle cell lymphoma. Blood 119(9):1963–1971

Kunisato A, Chiba S, Nakagami-Yamaguchi E et al (2003) HES-1 preserves purified hematopoietic stem cells ex vivo and accumulates side population cells in vivo. Blood 101(5):1777–1783

Kuroda K, Han H, Tani S et al (2003) Regulation of marginal zone B cell development by MINT, a suppressor of Notch/RBP-J signaling pathway. Immunity 18(2):301–312

Lee SY, Kumano K, Nakazaki K et al (2009) Gain-of-function mutations and copy number increases of Notch2 in diffuse large B-cell lymphoma. Cancer Sci 100(5):920–926

Lewis KL, Caton ML, Bogunovic M et al (2011) Notch2 receptor signaling controls functional differentiation of dendritic cells in the spleen and intestine. Immunity 35(5):780–791

Loder F, Mutschler B, Ray RJ et al (1999) B cell development in the spleen takes place in discrete steps and is determined by the quality of B cell receptor-derived signals. J Exp Med 190(1):75–89

Maekawa Y, Tsukumo S, Chiba S et al (2003) Delta1-Notch3 interactions bias the functional differentiation of activated CD4+ T cells. Immunity 19(4):549–559
Maekawa Y, Minato Y, Ishifune C et al (2008) Notch2 integrates signaling by the transcription factors RBP-J and CREB1 to promote T cell cytotoxicity. Nat Immunol 9(10):1140–1147
Maillard I, Koch U, Dumortier A et al (2008) Canonical notch signaling is dispensable for the maintenance of adult hematopoietic stem cells. Cell Stem Cell 2(4):356–366
Mancini SJ, Mantei N, Dumortier A, Suter U, MacDonald HR, Radtke F (2005) Jagged1-dependent Notch signaling is dispensable for hematopoietic stem cell self-renewal and differentiation. Blood 105(6):2340–2342
Martin F, Kearney JF (2002) Marginal-zone B cells. Nat Rev Immunol 2(5):323–335
Maruyama H, Yabu Y, Yoshida A, Nawa Y, Ohta N (2000) A role of mast cell glycosaminoglycans for the immunological expulsion of intestinal nematode, *Strongyloides venezuelensis*. J Immunol 164(7):3749–3754
Miller HR, Pemberton AD (2002) Tissue-specific expression of mast cell granule serine proteinases and their role in inflammation in the lung and gut. Immunology 105(4):375–390
Ohishi K et al. (2002) Delta-1 enhances marrow and thymus repopulating ability of human CD34(+)CD38(-) cord blood cells. J Clin Invest 110(8):1165–1174
Oyama T, Harigaya K, Muradil A et al (2007) Mastermind-1 is required for Notch signal-dependent steps in lymphocyte development in vivo. Proc Natl Acad Sci USA 104(23):9764–9769
Puente XS, Pinyol M, Quesada V et al (2011) Whole-genome sequencing identifies recurrent mutations in chronic lymphocytic leukaemia. Nature 475(7354):101–105
Radtke F, Wilson A, Stark G et al (1999) Deficient T cell fate specification in mice with an induced inactivation of Notch1. Immunity 10(5):547–558
Saito T, Chiba S, Ichikawa M et al (2003) Notch2 is preferentially expressed in mature B cells and indispensable for marginal zone B lineage development. Immunity 18(5):675–685
Sakata-Yanagimoto M, Nakagami-Yamaguchi E, Saito T et al (2008) Coordinated regulation of transcription factors through Notch2 is an important mediator of mast cell fate. Proc Natl Acad Sci USA 105(22):7839–7844
Sakata-Yanagimoto M, Sakai T, Miyake Y et al (2011) Notch2 signaling is required for proper mast cell distribution and mucosal immunity in the intestine. Blood 117(1):128–134
Sheng Y, Yahata T, Negishi N et al (2008) Expression of Delta-like 1 in the splenic non-hematopoietic cells is essential for marginal zone B cell development. Immunol Lett 121(1):33–37
Song R, Kim YW, Koo BK et al (2008) Mind bomb 1 in the lymphopoietic niches is essential for T and marginal zone B cell development. J Exp Med 205(11):2525–2536
Steinman RM, Idoyaga J (2010) Features of the dendritic cell lineage. Immunol Rev 234(1):5–17
Stier S, Cheng T, Dombkowski D, Carlesso N, Scadden DT (2002) Notch1 activation increases hematopoietic stem cell self-renewal in vivo and favors lymphoid over myeloid lineage outcome. Blood 99(7):2369–2378
Sugimoto K, Maekawa Y, Kitamura A et al (2010) Notch2 signaling is required for potent antitumor immunity in vivo. J Immunol 184(9):4673–4678
Sun J, Krawczyk CJ, Pearce EJ (2008) Suppression of Th2 cell development by Notch ligands Delta1 and Delta4. J Immunol 180(3):1655–1661
Suluki T et al. (2006) Highly efficient ex vivo expansion of human hematopoietic stem cells using Delta1-Fc chimeric protein. Stem Cells 24(11):2456–2465
Tan JB, Xu K, Cretegny K et al (2009) Lunatic and manic fringe cooperatively enhance marginal zone B cell precursor competition for delta-like 1 in splenic endothelial niches. Immunity 30(2):254–263
Tanigaki K, Han H, Yamamoto N et al (2002) Notch-RBP-J signaling is involved in cell fate determination of marginal zone B cells. Nat Immunol 3(5):443–450
Troen G, Wlodarska I, Warsame A, Hernandez Llodra S, De Wolf-Peeters C, Delabie J (2008) NOTCH2 mutations in marginal zone lymphoma. Haematologica 93(7):1107–1109
Tu L, Fang TC, Artis D et al (2005) Notch signaling is an important regulator of type 2 immunity. J Exp Med 202(8):1037–1042

Varnum-Finney B, Xu L, Brashem-Stein C et al (2000) Pluripotent, cytokine-dependent, hematopoietic stem cells are immortalized by constitutive Notch1 signaling. Nat Med 6(11):1278–1281

Varnum-Finney B, Halasz LM, Sun M, Gridley T, Radtke F, Bernstein ID (2011) Notch2 governs the rate of generation of mouse long- and short-term repopulating stem cells. J Clin Invest 121(3):1207–1216

Weng AP, Ferrando AA, Lee W et al (2004) Activating mutations of NOTCH1 in human T cell acute lymphoblastic leukemia. Science 306(5694):269–271

Wouters BJ, Jorda MA, Keeshan K et al (2007) Distinct gene expression profiles of acute myeloid/T-lymphoid leukemia with silenced CEBPA and mutations in NOTCH1. Blood 110(10):3706–3714

Wu L, Maillard I, Nakamura M, Pear WS, Griffin JD (2007) The transcriptional coactivator Maml1 is required for Notch2-mediated marginal zone B-cell development. Blood 110(10):3618–3623

Zweidler-McKay PA, He Y, Xu L et al (2005) Notch signaling is a potent inducer of growth arrest and apoptosis in a wide range of B-cell malignancies. Blood 106(12):3898–3906

c-Maf plays a crucial role for the definitive erythropoiesis that accompanies erythroblastic island formation in the fetal liver

Manabu Kusakabe,[1,2] Kazuteru Hasegawa,[1] Michito Hamada,[1] Megumi Nakamura,[1] Takayuki Ohsumi,[1] Hirona Suzuki,[1] Mai Thi Nhu Tran,[3] Takashi Kudo,[1] Kazuhiko Uchida,[4] Haruhiko Ninomiya,[2] Shigeru Chiba,[2] and Satoru Takahashi[1]

[1]Department of Anatomy and Embryology, Institute of Basic Medical Sciences, and [2]Department of Hematology, Institute of Clinical Medicine, Graduate School of Comprehensive Human Sciences, University of Tsukuba, Tsukuba, Ibaraki, Japan; [3]Laboratory of Stem Cell Research and Application, University of Science, Ho Chi Minh City, Vietnam; and [4]Department of Molecular Biological Oncology, Institute of Basic Medical Sciences, Graduate School of Comprehensive Human Sciences, University of Tsukuba, Tsukuba, Ibaraki, Japan

c-Maf is one of the large Maf (musculoaponeurotic fibrosarcoma) transcription factors that belong to the activated protein-1 super family of basic leucine zipper proteins. Despite its overexpression in hematologic malignancies, the physiologic roles c-Maf plays in normal hematopoiesis have been largely unexplored. On a C57BL/6J background, *c-Maf*$^{-/-}$ embryos succumbed from severe erythropenia between embryonic day (E) 15 and E18. Flow cytometric analysis of fetal liver cells showed that the mature erythroid compartments were significantly reduced in *c-Maf*$^{-/-}$ embryos compared with *c-Maf*$^{+/+}$ littermates. Interestingly, the CFU assay indicated there was no significant difference between *c-Maf*$^{+/+}$ and *c-Maf*$^{-/-}$ fetal liver cells in erythroid colony counts. This result indicated that impaired definitive erythropoiesis in *c-Maf*$^{-/-}$ embryos is because of a non–cell-autonomous effect, suggesting a defective erythropoietic microenvironment in the fetal liver. As expected, the number of erythroblasts surrounding the macrophages in erythroblastic islands was significantly reduced in *c-Maf*$^{-/-}$ embryos. Moreover, decreased expression of VCAM-1 was observed in *c-Maf*$^{-/-}$ fetal liver macrophages. In conclusion, these results strongly suggest that c-Maf is crucial for definitive erythropoiesis in fetal liver, playing an important role in macrophages that constitute erythroblastic islands. (*Blood*. 2011;118(5): 1374-1385)

Introduction

In mouse embryogenesis, red blood cells are produced in the yolk sac in a process called primitive erythropoiesis. Erythropoiesis then takes place in the fetal liver around embryonic day (E) 10 onward and in BM and spleen after birth. This process, which is characterized by enucleated red blood cells, is called definitive erythropoiesis.[1] During terminal erythroid differentiation, erythroblasts are associated with a central macrophage, which forms a specialized microenvironment, the so-called erythroblastic islands. In the erythroblastic islands, a central macrophage provides favorable proliferative and survival signals to the surrounding erythroblasts, and it eventually engulfs the extruded nuclei of maturing erythrocytes.[2-5] Inhibition of the interaction between macrophage and erythroblasts usually leads to embryonic anemia accompanied by accelerated apoptosis of erythroid cells. Targeted disruption of the gene *palld*, which encodes actin cytoskeleton associated protein (palladin) prevented effective erythroblast-macrophage interactions because of differentiation defects in the macrophage. Therefore, mouse embryos homozygous for the mutant gene experience severe anemia and succumb in the embryonic period.[6] Meanwhile, it has been reported that a series of adhesion molecules are also involved in the process of forming erythroblastic islands. Erythroblast macrophage protein (EMP) is a transmembrane protein expressed in both erythroblasts and macrophages, and it mediates the erythroblast-macrophage interaction. Indeed, the targeted deletion of EMP causes lethal anemia in mouse embryos because of the suppressed formation of erythroblastic islands.[7] Furthermore, a previous report showed that the interaction between very late Ag-4 ($\alpha_4\beta_1$ integrin) on erythroblasts and VCAM-1 on macrophages plays a key role in maintaining the islands.[8] For example, administration of Abs raised against either $\alpha_4\beta_1$ integrin or VCAM-1 caused disruption of the island structure.[8] However, the molecular mechanism, in terms of transcriptional regulation of island-affiliated genes in macrophages, remains largely unknown.

The large Maf transcription factor c-Maf is a cellular homolog of v-maf, which was isolated from a chicken musculoaponeurotic fibrosarcoma induced by avian retrovirus AS42 infection.[9] The large Maf transcription factors contain an acidic domain that promotes transcriptional regulation and a basic region/leucine zipper domain that mediates dimerization, as well as DNA binding to either Maf recognition elements (MAREs) or the 5′ AT-rich half-MARE.[10-12] Each large Maf protein has been shown to play a distinct role in cellular proliferation and differentiation in both pathologic and physiologic situations.[9,13-19] In B-lymphoid and T-lymphoid lineages, aberrant expression of c-Maf works as an oncogene, as shown in patients with multiple myeloma and angioimmunoblastic T-cell lymphoma and in a transgenic mouse model.[20-23] Physiologic c-Maf expression is indispensable for the proper regulation of IL-4 and IL-21 gene expression in T-helper cells.[24,25] In macrophages, c-Maf has been reported to regulate IL-10 expression, which is essential for differentiation of regulatory T cells.[26] In addition, combined deficiency of MafB and c-Maf

Submitted August 4, 2010; accepted May 3, 2011. Prepublished online as *Blood* First Edition paper, May 31, 2011; DOI 10.1182/blood-2010-08-300400.

An Inside *Blood* analysis of this article appears at the front of this issue.

The online version of the article contains a data supplement.

The publication costs of this article were defrayed in part by page charge payment. Therefore, and solely to indicate this fact, this article is hereby marked "advertisement" in accordance with 18 USC section 1734.

enables long-term expansion of differentiated, mature macrophages.[27] We recently reported that c-Maf is abundantly expressed in fetal liver macrophages and that it regulates expression of F4/80, which mediates immune tolerance.[28] However, the physiologic consequences of c-Maf deletion on terminal erythroid differentiation in erythroblastic islands have been largely unexplored.

In the present study, we demonstrate that *c-Maf*–deficient mice exhibit embryonic anemia, which is associated with a failure to retain erythroblastic islands. Moreover, we found significantly reduced expression of VCAM-1 in *c-Maf*–deficient macrophages, which presumably accounts for the deficiency in island maintenance and subsequent embryonic anemia. Thus, these results suggest that c-Maf is indispensable for definitive erythropoiesis in fetal liver, because it activates VCAM-1 expression in macrophages, and this causes the maintenance of erythroblastic islands.

Methods

Mice

c-Maf–deficient mice were originally generated on a 129/Sv background[14] and have been backcrossed onto a C57BL/6J background for > 7 generations. In staging the embryos, gestational day 0.5 (E0.5) was defined as noon of the day a vaginal plug was found after overnight mating. Mice were maintained in specific pathogen-free conditions in a Laboratory Animal Resource Center. All experiments were performed according to the Guide for the Care and Use of Laboratory Animals at the University of Tsukuba.

Hematologic analysis of fetal liver cells, embryonic blood, and adult blood

Single-cell suspensions prepared from fetal livers were washed and resuspended in 1 mL of 2% FBS/PBS. The cell number was counted with the use of a hemocytometer. Collection of embryonic peripheral blood was performed as described previously.[29] Peripheral blood samples from adult mice were obtained from retro-orbital venous plexus with the use of heparin-coated microtubes. Blood counts were determined with an automated hemocytometer (Nihon Kohden). Blood smears were prepared with the wedge technique and were stained with May-Grünwald-Giemsa and then photographed with a Keyence Biorevo BZ-9000 microscope. Images were processed with Photoshop software (Adobe).

Flow cytometry

Freshly isolated fetal liver cells were immunostained at 4°C in PBS/2% FBS in the presence of 5% mouse serum to block Fc receptors. Cells were incubated with FITC-conjugated anti–TER-119 and allophycocyanin (APC)–conjugated anti-CD44 Abs, followed by a 5-minute incubation with phycoerythrin PE-conjugated Annexin V (BioVision) at room temperature. To quantify the presence of VCAM-1 and integrin αV on macrophages, FITC-conjugated anti–Mac-1, Alexa Fluor 647–conjugated anti–VCAM-1 and PE-conjugated anti-integrin αV Abs were used for analyses. All Abs except PE-conjugated annexin V were from eBioscience. Flow cytometry was performed on a Becton Dickinson FACS LSR with CellQuest software. The isolation of erythroblasts at different stages of maturation was performed as described previously.[30] Data were analyzed with FlowJo (Tree Star Inc) analysis software.

Cell cycle analysis

Cell cycle analysis was performed with propidium iodide (PI). Further details are provided in supplemental Methods (available on the *Blood* website; see the Supplemental Materials link at the top of the online article).

Histology and TUNEL assay

Whole E13.5 embryos were fixed in 10% formalin neutral buffer solution (Wako). Paraffin-embedded tissue was sectioned, mounted, and stained with H&E. TUNEL assays were performed with an in situ Apoptosis Detection Kit according to the manufacturer's protocol (TaKaRa). Images were captured by a digital camera system with the use of a Leica DM RXA2 microscope (Leica Microsystems).

CFU assay

CFU assays were performed in MethoCult GF M3434 (StemCell Technologies) for erythroid burst-forming unit (BFU-E) and granulocyte, erythroid, megakaryocyte, and macrophage CFU (CFU-GEMM), and M3334 for erythroid CFU (CFU-E), following the manufacturer's instructions. CFU-E was scored 2 days after plating. BFU-E and CFU-GEMM were scored 8 days after plating.

Preparation of "native" erythroblastic islands and "reconstituted" erythroblastic islands

Native erythroblastic islands were isolated from fetal livers with the use of a previously described protocol.[31] Full details are provided in supplemental Methods.

Microarray analysis of fetal liver macrophages

Microarray analysis was performed as described previously.[32] Further details are provided in supplemental Methods. The data have been deposited in the Gene Expression Omnibus database under the accession number GSE23305.

Real-time RT-PCR analysis of fetal liver macrophages

Macrophages were prepared from fetal livers of *c-Maf*$^{+/+}$ or *c-Maf*$^{-/-}$ mice. Separation of fetal liver macrophages with the use of Mac-1^{+} magnetic beads and the MACS system was performed as described previously.[28] RNA extraction and quantitative RT-PCR were performed as described previously.[28] Primers used for PCR and the PCR conditions are available in supplemental Table 1.

Luciferase reporter assay

The *VCAM-1* 0.7 kilobase (kb) promoter (VCAM-1 Luc) or VCAM-1 mut Luc ligated to a luciferase reporter[33] was transiently cotransfected with c-Maf expression plasmids in macrophage cell line J774 with the use of FuGENE 6 (Roche). Twenty-four hours after the transfection, cells were collected, and reporter gene assays were performed with the Dual Luciferase Kit (Promega). Transfection efficiency was normalized to the expression of *Renilla* luciferase.

Reconstitution of hematopoietic system with fetal liver cells

The donor cells for hematopoietic reconstitution were prepared from E14.5 fetal livers of *c-Maf*$^{+/+}$ or *c-Maf*$^{-/-}$ (C57BL/6J-Ly5.1) mice. Fetal liver cells (2×10^6 cells) were injected into the tail vein of 8- to 10-week-old C57BL/6J-Ly5.2 mice that were previously exposed to x-rays at a 10-Gy dose.

Phenylhydrazine stress test

Mice were injected subcutaneously on days 0, 1, and 3 with 50 mg/kg phenylhydrazine (PHZ) hydrochloride solution in PBS as previously described.[34] Blood was obtained from the retro-orbital plexus on days 0, 3, 6, 8, and 10.

Statistical analysis

Data were represented as mean ± SEM. Statistical significance between any 2 groups was determined by the 2-tailed Student *t* test, in which *P* values < .05 were considered significant.

Table 1. Genotypic analysis of neonates and embryos from *c-Maf*$^{+/-}$ intercross on a C57BL/6J background

Embryonic stage	No. of each *c-Maf* genotype (no. of dead embryos)			Total no. of embryos
	c-Maf$^{+/+}$	*c-Maf*$^{+/-}$	*c-Maf*$^{-/-}$	
E12.5	13	30	15	58
E13.5	57	88	46 (5)	191
E14.5	75	135	55 (12)	265
E15.5	35	58	16 (3)	109
E16.5	11	15	4 (3)	30
E18.5	14	18	4 (3)	36
Neonate	13	29	0	42

Embryos were isolated at the indicated time points of gestation and within 7 days of birth (postnatal), and analyzed for viability. Genotypes of embryos were determined by PCR.

Results

Lethal erythropoietic deficiency in *c-Maf*$^{-/-}$ embryos

The *c-Maf*$^{-/-}$ mice, as originally generated, exhibited perinatal mortality within a few hours after birth on a 129/Sv background.[14] However, unexpectedly, on a C57BL/6J genetic background, c-Maf deficiency resulted in embryonic lethality from E15.5 onward, and almost all *c-Maf*$^{-/-}$ embryos died before E18.5 (Table 1). The fetal livers from *c-Maf*$^{-/-}$ embryos at E13.5 appeared pale compared with those from healthy *c-Maf*$^{+/+}$ control embryos (Figure 1A). As expected, the hematocrits of peripheral blood in the *c-Maf*$^{-/-}$ embryos (E13.5~E15.5) were markedly reduced (E13.5. 13.4% ± 1.8%; E14.5, 14.5% ± 1.0%; E15.5, 16.9% ± 1.0%), compared with the *c-Maf*$^{+/+}$ controls (E13.5, 18.7% ± 0.6%; E14.5, 23.1% ± 1.7%; E15.5, 29.6% ± 1.8%; Figure 1B). May-Grünwald-Giemsa staining of peripheral blood smears showed a significant reduction of enucleated red blood cells in *c-Maf*$^{-/-}$ embryos (E13.5, 6.68% ± 1.0%; E14.5, 17.2% ± 1.9%; E15.5, 29.8% ± 5.6%; Figure 1C-D), whereas *c-Maf*$^{+/+}$ control embryos retained a normal population of enucleated red blood cells (E13.5, 25.5% ± 4.7%; E14.5, 54.1% ± 1.1%; E15.5, 86.9% ± 2.8%; Figure 1C-D). Considering that the enucleated red blood cells are mainly derived from definitive erythropoiesis, these data suggest that c-Maf–deficient embryos suffer from impaired definitive erythropoiesis on the C57BL/6J genetic background. A previous study showed that placental insufficiency causes embryonic lethality.[35] To assess the effect of c-Maf on the placenta, immunofluorescence staining of placenta was performed with an anti–c-Maf Ab (supplemental Figure 1B). The expression of c-Maf was not detected in placenta. Compared with the head tissue as a positive control, c-Maf mRNA expression was 5-fold less in the placenta (supplemental Figure 1C). In addition, no obvious abnormalities in the *c-Maf*$^{-/-}$ placenta were observed after H&E staining (supplemental Figure 1D).

Increased apoptotic cell death in *c-Maf*$^{-/-}$ fetal liver

We next examined the cellular viability, as well as the cell cycle status, of *c-Maf*$^{-/-}$ fetal liver cells, in the hope of elucidating the molecular and cellular basis of their erythropoietic deficiency. The fetal liver size in *c-Maf*$^{-/-}$ embryos was smaller; thus, consistently fewer fetal liver cells were harvested from *c-Maf*$^{-/-}$ embryos between E13.5 and E15.5 (E13.5, 3.37 ± 0.5 × 10^6 cells; E14.5, 7.61 ± 1.0 × 10^6 cells; E15.5, 6.54 ± 2.7 × 10^6 cells) than from age-matched *c-Maf*$^{+/+}$ control embryos (E13.5, 6.89 ± 0.4 × 10^6 cells; E14.5, 16.6 ± 2.3 × 10^6 cells; E15.5, 32.5 ± 2.4 × 10^6 cells; Figure 2A-B). Of note, H&E staining of E13.5 *c-Maf*$^{-/-}$ fetal liver sections showed an increased number of pyknotic nuclei, which are indicative of apoptosis, compared with the *c-Maf*$^{+/-}$ control embryo (Figure 2C). In addition, TUNEL-positive apoptotic cells were remarkably increased in E13.5 *c-Maf*$^{-/-}$ fetal liver sections (Figure 2C). Moreover, flow cytometric analysis of PI-stained fetal liver cells showed an increased abundance of a sub-G_0/G_1 population early apoptotic cell fraction in *c-Maf*$^{-/-}$ fetal liver (8.77% ± 2.5%) compared with *c-Maf*$^{+/+}$

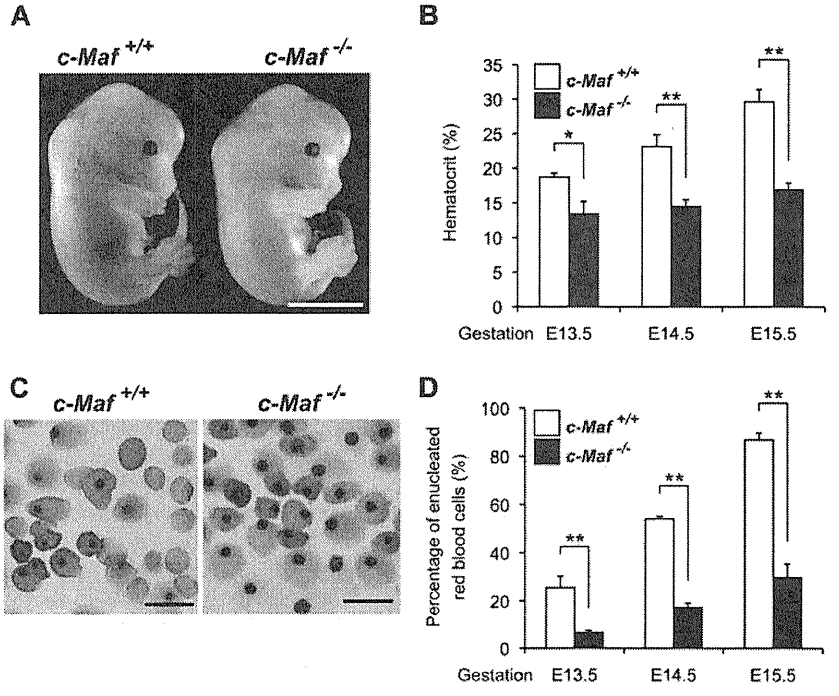

Figure 1. *c-Maf*$^{-/-}$ embryos are anemic. (A) Gross appearance of E13.5 embryos. The *c-Maf*$^{-/-}$ embryo is paler and smaller than its *c-Maf*$^{+/+}$ littermate. Scale bar represents 5 mm. The picture was taken with a NIKON coolpix 5200 digital camera in macro mode and processed with the Adobe Photoshop CS4 software. (B) Hematocrit values for *c-Maf*$^{+/+}$ (n = 6) and *c-Maf*$^{-/-}$ (n = 6) embryos at E13.5, *c-Maf*$^{+/+}$ (n = 8) and *c-Maf*$^{-/-}$ (n = 7) embryos at E14.5, and *c-Maf*$^{+/+}$ (n = 12) and *c-Maf*$^{-/-}$ (n = 9) embryos at E15.5. Data are presented as mean ± SEM. The mean hematocrit values for *c-Maf*$^{-/-}$ embryos were significantly lower than values for *c-Maf*$^{+/+}$ at E13.5, E14.5, and E15.5. (C) Blood smears from E13.5 embryos stained with May-Grünwald-Giemsa stain. The blood smear from a *c-Maf*$^{-/-}$ embryo contains far fewer enucleated red blood cells. Images were acquired by a Biorevo BZ microscope (Plan Apo 20×0.75 DIC N2) at room temperature and processed with the Adobe Photoshop CS4 software. Scale bars represent 20 μm. (D) The percentage of enucleated red blood cells in peripheral blood for *c-Maf*$^{+/+}$ (n = 5) and *c-Maf*$^{-/-}$ (n = 7) embryos at E13.5, *c-Maf*$^{+/+}$ (n = 4) and *c-Maf*$^{-/-}$ (n = 4) embryos at E14.5, and *c-Maf*$^{+/+}$ (n = 8) and *c-Maf*$^{-/-}$ (n = 8) embryos at E15.5. A minimum of 200 cells was counted for each sample. Data are presented as mean ± SEM. The percentage of enucleated red blood cells is significantly reduced in *c-Maf*$^{-/-}$ embryos than in *c-Maf*$^{+/+}$ embryos at E13.5, E14.5, and E15.5. *$P < .05$ and **$P < .01$.

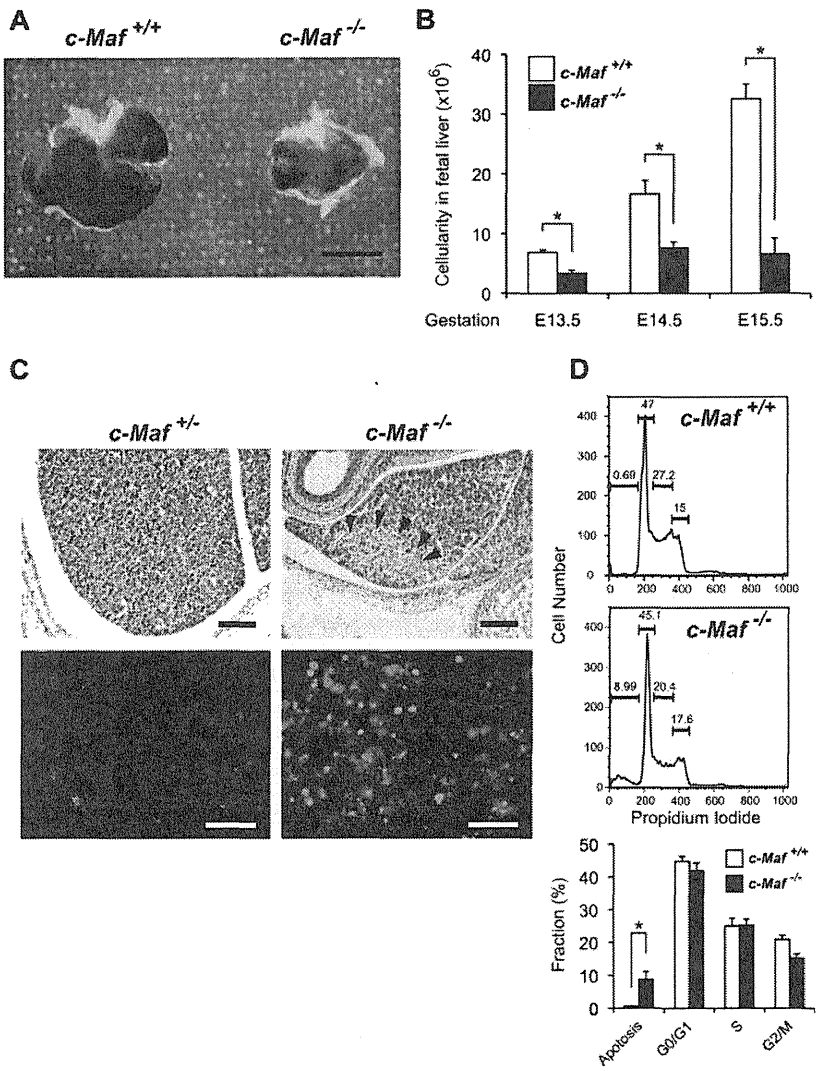

Figure 2. Increased number of apoptotic cells is observed in *c-Maf*$^{-/-}$ fetal liver. (A) Gross appearance of E13.5 fetal liver. The *c-Maf*$^{-/-}$ fetal liver is smaller than a *c-Maf*$^{+/+}$ fetal liver. Scale bar represents 100 μm. The picture was taken with a NIKON coolpix 5200 digital camera in macro mode and processed with the Adobe Photoshop CS4 software.(B) The mean total number of fetal liver cells in *c-Maf*$^{+/+}$ (n = 14) and *c-Maf*$^{-/-}$ (n = 10) embryos at E13.5, *c-Maf*$^{+/+}$ (n = 6) and *c-Maf*$^{-/-}$ (n = 4) embryos at E14.5, and *c-Maf*$^{+/+}$ (n = 8) and *c-Maf*$^{-/-}$ (n = 8) embryos at E15.5. The mean number of fetal liver cells is significantly reduced in *c-Maf*$^{-/-}$ embryos. Data are presented as mean ± SEM. (C) H&D staining of *c-Maf*$^{+/-}$ and *c-Maf*$^{-/-}$ fetal liver sections (top). Arrowheads indicate pyknotic nuclei, which indicate apoptotic cells. TUNEL assays showed increased apoptosis in the *c-Maf*$^{-/-}$ fetal liver (bottom panel). Images were acquired by a Leica DM RXA2 microscope (Lecia HC PL Fluotar 20×/0.50 PH2) at room temperature and processed with the Adobe Photoshop CS4 software. Scale bars in the top panel represent 200 μm. Scale bars in the bottom panel represent 50 μm. (D) The fraction of cells in different phases of the cell cycle was measured by PI staining followed by flow cytometric analyses. The percentage of cells in sub-G_0/G_1, G_1, S phase, and G_2/M are indicated. The sub-G_0/G_1 phase represents the apoptotic population. The apoptotic population was increased in *c-Maf*$^{-/-}$ fetal liver.

control cells (0.67% ± 0.01%; Figure 2D). However, the cellular population of each phase of the cell cycle, that is, G_0/G_1, S, and G_2/M, was not significantly affected (Figure 2D). Overall, these observations suggest that the fetal liver hematopoietic cells from *c-Maf*$^{-/-}$ embryos are prone to undergo apoptotic cell death.

Impaired fetal liver erythropoiesis because of a non–cell-autonomous effect of c-Maf deficiency

Given the significant disturbance of erythropoiesis, we next attempted to delineate the maturation status of erythroid lineage cells in *c-Maf*$^{-/-}$ fetal liver. To this end, we examined fetal liver erythropoiesis by flow cytometry with the use of the erythroid markers CD44 and TER-119, which distinguish various stages of erythroid-cell differentiation (Figure 3A). By modifying a method reported by Chen et al[30] to isolate erythroblasts at different maturation stages from adult BM, we isolated erythroblasts from fetal liver cells and analyzed their structure (Figure 3B). Decreased numbers of mature erythroid compartments (regions II, III, IV, and V in Figure 3C) were observed in *c-Maf*$^{-/-}$ fetal liver than in *c-Maf*$^{+/+}$ fetal liver. These results showed a reduction of basophilic erythroblasts, polychromatic erythroblasts, orthochromatic erythroblasts, reticulocytes, and mature red cells in *c-Maf*$^{-/-}$ fetal liver. Previously, Zhang et al[36] reported a method to study erythropoiesis with the use of an anti-CD71 Ab and an anti–TER-119 Ab. Similar results were obtained with their method. Decreased numbers of mature erythroid compartments (region 3 to region 5 in supplemental Figure 2A-B) were observed in *c-Maf*$^{-/-}$ fetal liver in combination with anti-CD71 Ab and anti–TER-119 Ab. These observations prompted us to quantify the apoptotic cell population at each stage of erythroid cells by annexin V staining.

In good agreement with the preferential decrease of the mature erythroid compartments (regions II-V), we observed a highly increased number of annexin V-positive cells in the most mature erythroid compartment (region V) of *c-Maf*$^{-/-}$ fetal liver compared with the *c-Maf*$^{+/+}$ fetal liver. In contrast, the premature erythroid compartments (regions I-IV) of *c-Maf*$^{-/-}$ fetal liver cells exhibited a comparable number of annexin V-positive cells with the *c-Maf*$^{+/+}$ control (Figure 3D; supplemental Figure 2C). To examine the state of globin regulation, the Mac-1$^-$ cells from E13.5 fetal liver were sorted and analyzed for mRNA of Hbb (hemoglobin beta chain) genes by real-time RT-PCR analysis. Expression profiles showing switching of Hbb genes indicated that the definitive Hbb gene Hbb-b1 (hemoglobin, beta adult major chain) was significantly down-regulated, whereas the primitive globin genes Hbb-bH1

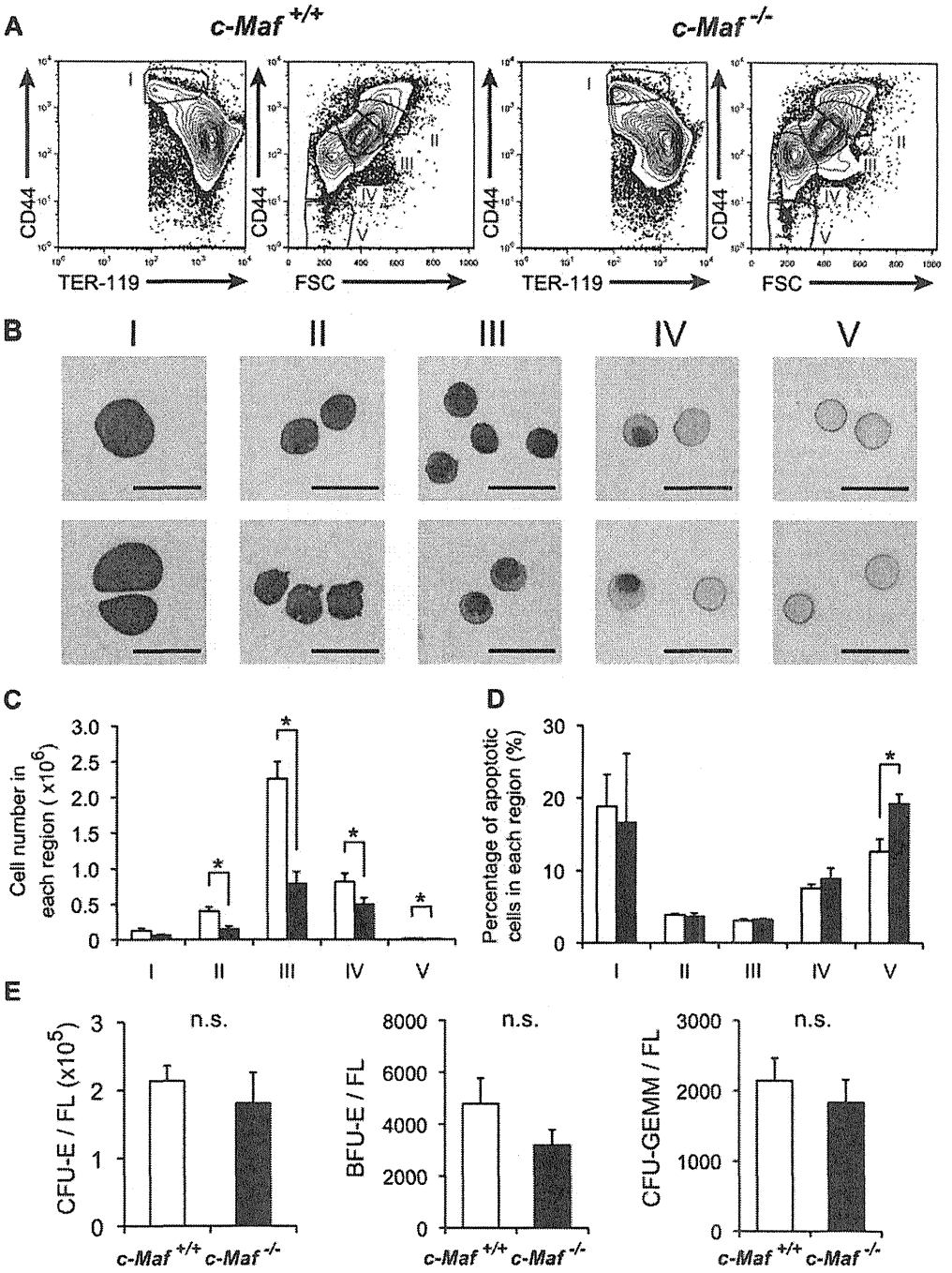

Figure 3. Definitive erythropoiesis in fetal liver is impaired in *c-Maf*$^{-/-}$ embryos but *c-Maf*$^{-/-}$ fetal liver cells can form erythroid colonies. (A) Flow cytometric analysis of fetal liver cells isolated from E13.5 embryos labeled with a FITC-conjugated anti–TER-119 mAb and an APC-conjugated anti-CD44 mAb. Regions I to V are defined by a characteristic staining pattern and forward scatter (FSC) intensity of cells as indicated. (B) Representative images of erythroblast structure on stained cytospins from the 5 distinct regions shown in Figure 3A of wild-type fetal liver. Images were acquired by a Biorevo BZ microscope (Plan Apo 20×0.75 DIC N2) at room temperature and processed with the Adobe Photoshop CS4 software. Scale bar represents 20 μm. (C) Comparison of *c-Maf*$^{+/+}$ and *c-Maf*$^{-/-}$ fetal livers in region I to region V. □ represents *c-Maf*$^{+/+}$; ■, *c-Maf*$^{-/-}$; n = 8~10 per group; *$P < .05$. (D) The ratio of annexin V$^+$ cells from region I to region V was compared in *c-Maf*$^{+/+}$ and *c-Maf*$^{-/-}$ fetal livers. □ represents *c-Maf*$^{+/+}$; ■, *c-Maf*$^{-/-}$; n = 3 per group; *$P < .05$. (E) In vitro colony assay with the use of fetal liver cells from *c-Maf*$^{+/+}$ (□) and *c-Maf*$^{-/-}$ (■) embryos at E13.5. A total of 20 000 fetal liver cells were plated and cultured with methylcellulose media. The numbers of CFU-E–, BFU-E–, and CFU-GEMM–derived colonies per fetal liver are shown. No significant difference (n.s.) was found in the number of CFU-E–, BFU-E–, or CFU-GEMM–derived colonies per fetal liver in *c-Maf*$^{+/+}$ embryos and *c-Maf*$^{-/-}$ embryos; n = 6~7 per group; data are presented as mean ± SEM. FL indicates fetal liver.

(hemoglobin z, beta-like embryonic chain) and Hbb-y (hemoglobin y, beta-like embroyonic chain) were not significantly suppressed in the *c-Maf*$^{-/-}$ fetal liver erythroid fraction compared with the *c-Maf*$^{+/+}$ control (supplemental Figure 3).

To examine the colony formation potential of hematopoietic progenitors in *c-Maf*$^{-/-}$ fetal liver, conventional set of CFU assays were performed. As a result of CFU assays, there were no significant differences between *c-Maf*$^{+/+}$ and *c-Maf*$^{-/-}$ in the

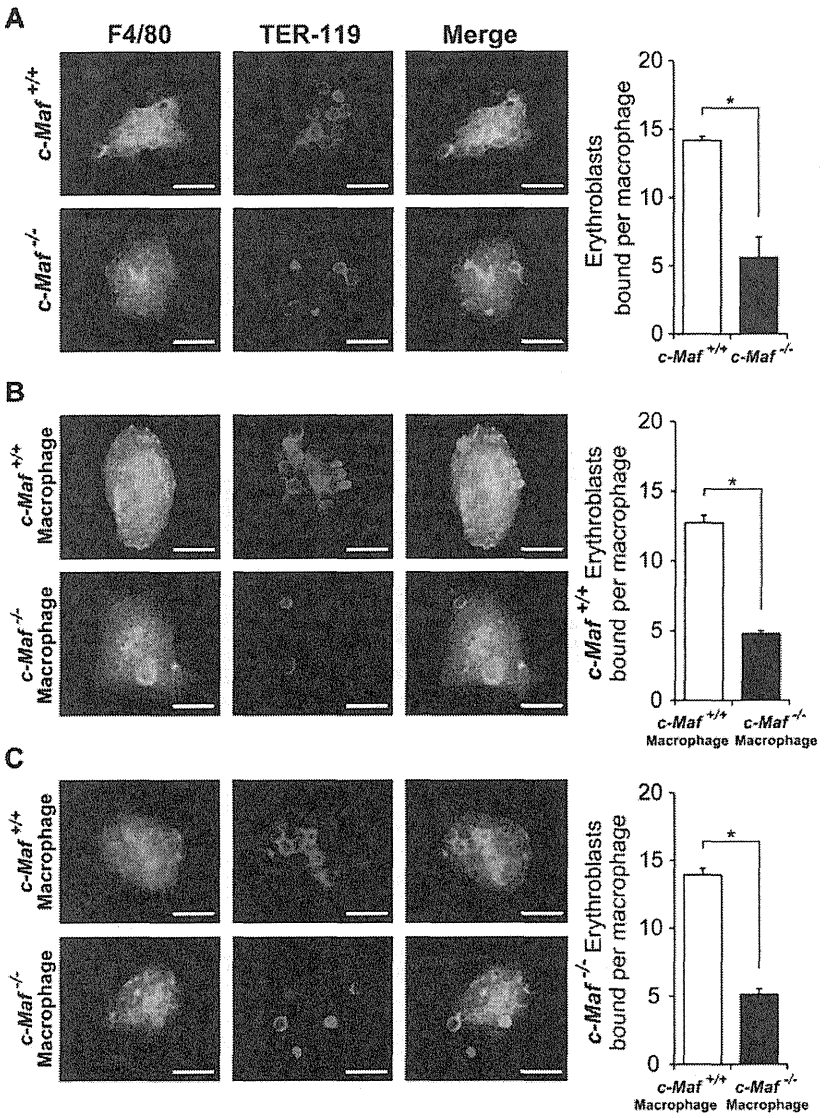

Figure 4. Absence of c-Maf impairs the formation of erythroblastic islands in the fetal liver. (A) Native erythroblastic islands isolated from *c-Maf*$^{+/+}$ and *c-Maf*$^{-/-}$ fetal liver were immunostained with F4/80 (green) and TER-119 (red) Abs as described in "Methods." F4/80 is used as a macrophage-specific marker, and TER-119 is used as a marker for erythroblasts. The number of erythroblasts surrounding each macrophage was significantly reduced in *c-Maf*$^{-/-}$ fetal liver. (B) Erythroblastic islands reconstituted with *c-Maf*$^{+/+}$ erythroblasts were immunostained. The number of *c-Maf*$^{+/+}$ erythroblasts surrounding each *c-Maf*$^{+/+}$ or *c-Maf*$^{-/-}$ macrophage is shown. *c-Maf*$^{+/+}$ erythroblasts surrounding *c-Maf*$^{-/-}$ macrophages were significantly reduced compared with those seen for *c-Maf*$^{+/+}$ macrophages. (C) Erythroblastic islands reconstituted with *c-Maf*$^{-/-}$ erythroblasts were immunostained. The number of *c-Maf*$^{-/-}$ erythroblasts surrounding each *c-Maf*$^{+/+}$ or *c-Maf*$^{-/-}$ macrophage is shown. *c-Maf*$^{-/-}$ erythroblasts surrounding *c-Maf*$^{-/-}$ macrophage were significantly reduced compared with those seen for *c-Maf*$^{+/+}$ macrophages. Although *c-Maf*$^{-/-}$ erythroblasts can form reconstituted erythroblastic islands with *c-Maf*$^{+/+}$ macrophages, *c-Maf*$^{-/-}$ macrophages showed impaired formation of reconstituted erythroblastic islands with *c-Maf*$^{+/+}$ erythroblasts. Images were acquired by a Biorevo BZ microscope (Plan Apo 20×0.75 DIC N2) at room temperature and processed with the Adobe Photoshop CS4 software. The scale bar represents 20 μm; n = 4–6 embryos per group. For each combination, ≥ 20 macrophages per embryo were analyzed. *$P < .05$. Data are presented as mean ± SEM.

number of CFU-E–, BFU-E–, and CFU-GEMM–derived colonies per fetal liver (Figure 3E). In addition, CFU-E colonies were indistinguishable in structure and size (supplemental Figure 4A-B). Moreover, erythroid cells derived from *c-Maf*$^{-/-}$ CFU-Es exhibited a similar structure, and enucleated red blood cells were also similar to those from *c-Maf*$^{+/+}$ control CFU-Es in cytospin slides stained with May-Grünwald-Giemsa (supplemental Figure 4C). Taken together, these results suggest that *c-Maf*$^{-/-}$ erythroid cells are still capable of developing into mature cells in vitro, in contrast to the result of flow cytometric analysis with the use of fetal liver cells (Figures 3A-C; supplemental Figure 2A-B), which reflects the in vivo condition. Therefore, the impaired definitive erythropoiesis in the *c-Maf*$^{-/-}$ embryos is more likely because of a non–cell-autonomous effect of c-Maf deficiency.

Absence of c-Maf causes impaired erythroblastic island formation in the fetal liver

c-Maf is abundantly expressed in fetal liver macrophages, although it is largely missing from the erythroid cells in fetal liver. Therefore, we initially surmised that c-Maf deficiency in fetal liver macrophages disturbed the erythroblastic islands.[3] To address this hypothesis, we attempted to examine whether *c-Maf*$^{-/-}$ macrophages failed to maintain the erythroblastic islands. For this purpose, we isolated the erythroblastic island from *c-Maf*$^{+/+}$ and *c-Maf*$^{-/-}$ fetal livers and counted the number of erythroblasts associated with each single central macrophage according to a previously described method.[31]

Interestingly, although > 10 TER-119^{+} erythroblasts were adhered to a F4/80^{+} macrophage in *c-Maf*$^{+/+}$ fetal livers, c-Maf–deficient central macrophages seemed to harbor far fewer erythroblasts (Figure 4). As shown in Figure 4A, the number of erythroblasts attached to a single central macrophage was significantly reduced in *c-Maf*$^{-/-}$ erythroblastic islands (14.2 ± 0.3 and 5.6 ± 1.5 erythroblasts per macrophage for *c-Maf*$^{+/+}$ and *c-Maf*$^{-/-}$, respectively). This result clearly indicates that erythroblastic islands are impaired in the *c-Maf*$^{-/-}$ fetal livers.

Next, to address whether c-Maf deficiency in macrophages was specifically responsible for the impairment of erythroblastic islands, a series of reconstitution experiments was performed. After attaching native erythroblastic islands either from *c-Maf*$^{+/+}$ or *c-Maf*$^{-/-}$ fetal livers on a glass coverslip, the adherent erythroblasts in the islands were stripped from the macrophages. Next, the